SARCOCYSTIS CAFFERI, N. SP. (PROTOZOA: APICOMPLEXA) FROM THE AFRICAN BUFFALO (*SYNCERUS CAFFER*)

J. P. Dubey, Emily P. Lane*, Erna van Wilpe†, Essa Suleman*, Bjorn Reininghaus‡, S. K. Verma, B. M. Rosenthal, and Moses S. Mtshali*§

U. S. Department of Agriculture, Agricultural Research Service, Beltsville Agricultural Research Center, Animal Parasitic Diseases Laboratory, Building 1001, Beltsville, Maryland 20705-2350. Correspondence should be sent to: *jitender.dubey@ars.usda.gov*

*Research and Scientific Services Department, National Zoological Gardens of South Africa, Pretoria, 0001, South Africa.

†Department of Anatomy and Physiology, Faculty of Veterinary Science, University of Pretoria, Onderstepoort, 0110, South Africa.

‡Department of Agriculture, Fisheries and Forestry, Orpen, 1365, South Africa.

§Department of Zoology and Entomology, University of the Free State, Private Bag X13, Phuthaditjhaba, 9866, South Africa.

Abstract: *Sarcocystis* infections have been reported from the African buffalo (*Syncerus caffer*), but the species have not been named. Here we propose a new name *Sarcocystis cafferi* from the African buffalo. Histological examination of heart (92), skeletal muscle (36) and tongue (2) sections from 94 buffalos from the Greater Kruger National Park, South Africa, and a review of the literature revealed only 1 species of *Sarcocystis* in the African buffalo. Macrocysts were up to 12 mm long and 6 mm wide and were located in the neck muscles and overlying connective tissue. They were pale yellow; shaped like a litchi fruit stone or cashew nut; turgid or flaccid and

oval to round (not fusiform). By light microscopy (LM) the sarcocyst wall was relatively thin. By scanning electron microscopy (SEM), the sarcocyst wall had a mesh-like structure with irregularly shaped villar protrusions (vp) that were of different sizes and folded over the sarcocyst wall. The entire surfaces of vp were covered with papillomatous structures. By transmission electron microscopy (TEM), the sarcocyst wall was up to 3.6 μm thick and had highly branched villar protrusions that were up to 3 μm long. The villar projections contained filamentous tubular structures, most of which were parallel to the long axis of the projections but some tubules criss-crossed, especially at the base. Granules were absent from these tubules. Longitudinally cut bradyzoites were 12.1x 2.7 μm in size,had a long convoluted mitochondrion, and only 2 rhoptries. Phylogenetic analysis of *18S rRNA* and Cytochrome C oxidase subunit 1 (*cox1*) gene sequences indicated that this *Sarcocystis* species is very closely related to, but distinct from, *S. fusiformis and S. hirsuta*. Thus, morphological findings by LM, SEM and TEM together with molecular phylogenetic data (from *18S rRNA* and *cox1*) confirm that the *Sarcocystis* species in the African buffalo is distinct from *S. fusiformis* and has therefore been named *Sarcocystis cafferi.*

Species of *Sarcocystis* usually have a 2-host, prey-predator life cycle, with herbivores as intermediate hosts and carnivores as definitive hosts (Dubey et al., 1989). The intermediate host becomes infected with *Sarcocystis* species by ingesting sporocysts or oocysts, or both, excreted in the feces of the definitive host. After a brief period of schizogony, the parasite encysts in tissues and forms sarcocysts. The definitive host becomes infected by ingesting sarcocysts encysted in tissues of intermediate hosts.

Four species of *Sarcocystis* are currently recognized in the Asian water buffalo (*Bubalus bubalis*): *Sarcocystis fusiformis* and *Sarcocystis buffalonis* have macrocysts and cats act as

definitive hosts; *Sarcocystis levinei* has microcysts and dogs act as definitive host; *Sarcocystis dubeyi* has microcysts with an unknown definitive host (Dubey et al., 2014a). Of all the *Sarcocystis* species in cattle and buffaloes, *S. fusiformis* is biologically and morphologically distinctive; its sacrocysts are up to 25 mm long, fusiform in shape, typically occurs in esophagus of buffaloes, and cat is the definitive host. There is no morphological equivalent of *S. fusiformis* in cattle (Dubey et al., 1989; Dubey et al., 2014a,b).

Sarcocystis infections have been reported also from the African buffalo (*Syncerus caffer*) but the species have not been named. Quandt et al. (1997) first described the structure of the sarcocysts in the African buffalo, and reviewed earlier reports from this host. Kaliner et al. (1971, 1974), and Kaliner (1975) found sarcocysts in 14 buffaloes from Tanzania and Kenya, but did not describe the structure. Quandt et al. (1997) also mentioned unpublished records of sarcocysts in *S. caffer* from Uganda. Basson et al. (1970) recorded parasites in 97 buffalos from the Kruger National Park killed in 1966. Sarcocysts were found in 86 (94.5%) of 91 buffalos older than 1 yr of age but not in 6 animals less than 1 yr old. These observations were based on the presence of grossly visible macrocysts.

Quandt et al. (1997) critically examined tongues/esophagi of 40 African buffalos from the Kruger National Park but the year of sampling was not stated. Sarcocysts were detected in the tongues of 22 (66.6%) of 33 older animals (1-9 yr old) but not any of 7 young animals (7-10 mo old); the esophagus of 2 of these animals examined was also positive. They described the structure of sarcocyst but did not name it.

Here, we describe and propose a new name, *S. cafferi* for the *Sarcocystis* in the African buffalo.

MATERIALS AND METHODS

Naturally infected buffalos

Tissues of 2 African buffalos that died recently at the Greater Kruger National Park, Pretoria, 0001, South Africa were routinely examined at necropsy. For the present study, grossly visible sarcocysts from neck and overlying connective tissue evident during necropsy were examined from an African buffalo (#1) from the Greater Kruger National Park. Half of each macroscopically visible sarcocysts found in a second buffalo (#2) were preserved in 10% formalin for histological examination and the other half in 70% alcohol for DNA extraction. Affected muscle sections from both buffalo preserved in formalin were processed routinely for histopathology examination and stained with hematoxylin and eosin (H and E).

Retrospectively, H and E stained sections of hearts (92), skeletal muscle (34), and tongues (2) from 92 African buffalo cases submitted previously for routine diagnostic histopathology were also examined.

Scanning electron microscopy (SEM)

Part of a formalin-fixed sarcocyst was post-fixed in 1% osmium tetroxide in Millonig's buffer (pH 7.4), dehydrated through a series of graded ethanols into 100% ethanol. The absolute ethanol was substituted with liquid carbon dioxide and the samples critically point dried (E3100 Critical Point Drier, Quorum Technologies, Kent, UK), carbon coated and examined in a Zeiss Ultra Plus 55 FE-SEM (Carl Zeiss International, Oberkoch, Germany) operated at 1 kV.

Transmission electron microscopy (TEM)

Formalin-fixed muscle tissue from animal # 1 was processed for TEM using standard techniques. Briefly, the samples were post-fixed in 1% osmium tetroxide in Millonig's buffer (pH 7.4), dehydrated through a series of graded ethanols, infiltrated with an epoxy

resin/propylene oxide mixture before being embedded in absolute resin and polymerised at 60 C overnight. Ultrathin resin sections of 3 macrocysts were contrasted with uranyl acetate and lead citrate and examined in a Philips CM10 transmission electron microscope (FEI, Eindhoven, The Netherlands) operated at 80kV. Toluidine blue-stained resin sections were photographed with an Olympus BX63 compound microscope (Olympus, Wirsam, South Africa).

DNA extraction

Macrocysts (10 samples) preserved in alcohol were obtained from animal #2. A muscle tissue sample without any cysts from the same animal was used as a negative control. DNA was extracted from approximately 50 mg of tissue using the ZR Genomic DNA Tissue MiniPrep Kit (Zymo Research, Irvine, California) according to manufacturer's instructions. DNA concentration and quality was assessed using the NanoDrop ND-1000 spectrophotometer (NanoDrop Technologies Inc., Wilmington, Delaware).

PCR

An ~1.6 kb region of the *18S rRNA* gene was amplified by PCR according to Rosenthal et al. (2008). Briefly, primers 18S1F (GGATAACCGTGGTAATTCTATG) and 18S10R (AGCATGACGTTTTCCTATCTCTA) were used to amplify fragment 18S1a (~1086 bp corresponding to the *Toxoplasma gondii* homologue, EF472967) from each sample Yang et al., 2001a, 2001b; Rosenthal et al., 2008). Primers 18S7F (GGCTTGTCGCCTTGAATACTGC) and SSU-EUK (TGATCCTTCTGCAGGTTCACCTAC) were used to amplify fragment 18S1b (~1,012 bp) which partially overlaps the 18S1a amplicon (Medlin et al., 1988; Rosenthal et al., 2008). Furthermore an ~1 kb region of the mitochondrial cytochrome c oxidase subunit I (*cox1*) gene was amplified according to Gjerde (2013). Briefly, primers SF1 (ATGGCGTACAACAATCATAAAGAA) and CoxS1R

(TTACCCATGACCACACCTGTAGTACC) were used to amplify a region of the *Sarcocystis cox1* gene from each sample.

Each 25µl reaction contained 1 × KAPA HiFi HotStart ReadyMix (KAPA Biosystems, Cape Town, South Africa), 1µM of each primer, nuclease free water and 50ng of template DNA. PCR was performed on a Bio-Rad T100 Thermal Cycler (Bio-Rad Laboratories, Johannesburg, South Africa) according to the following thermal conditions: 95 C for 5 min followed by 35 cycles at 98 C for 30 sec, 53 C (*18S rRNA*) or 55 C (*cox1*) for 30 sec and 72 C for 90 sec. This was followed by a final extension at 72 C for 10 min. No-template controls were included in each run. PCR products were electrophoresed on 1.5% agarose gels stained with GRGreen dye (Thermo Fisher Scientific, Waltham, Massachusetts) in 1 × TAE buffer for 45 min at 100V and visualised on the Gel-Doc EZ System (Bio-Rad Laboratories).

Sequencing and phylogenetic analysis

The amplified *18s rRNA* and *cox1* gene fragments were purified and sequenced in both directions on the ABI 3130 XL Genetic Analyzer (Applied Biosystems, Johannesburg, South Africa). Sequence chromatograms were edited using the FinchTV software (Geospiza Inc., Seattle, Washington). Gene fragments (*18S* and *cox1*) were assembled using ContigExpress in Vector NTI Advance 11 (Life Technologies, New York City, New York). Multiple sequence alignment was performed on the assembled fragments (*18S* and *cox1*) for both the forward and reverse sequences to determine if the macrocysts belonged to the same *Sarcocystis* species. Furthermore, sequences (*18S rRNA* and *cox1*) from macrocyst samples were submitted to GenBank.

Phylogenetic analysis was performed using *S. cafferi 18S rRNA* (GenBank Accession numbers: KJ778010 to KJ778019) and *cox1* sequences (GenBank Accession numbers: KJ778020

to KJ778028) in MEGA 5.2 (Tamura et al., 2011), according to the procedure described by Hall (2013). Briefly, *18S rRNA* sequences of the 100 closest homologues identified by BLAST analysis of the 1682bp *18S rRNA* sequence (GenBank Accession Number: KJ778012) were selected from GenBank for further analysis. Multiple sequence alignment was performed in MEGA using the MUSCLE algorithm (Edgar, 2004a, 2004b). The Maximum Likelihood algorithm was used to compute the best model for estimation of the phylogenetic tree. The phylogenetic tree was constructed in MEGA under the criterion of maximum likelihood using the HKY85 model (Hasegawa et al., 1985) with the invariant rates among sites parameter selected and reliability of the generated tree evaluated by bootstrapping analysis set to 500 replicates (Felsentein, 1985). Thereafter, the sequence alignment was re-analyzed and 42 sequences having the closest homology to *S. cafferi*, (corresponding to positions 1 to 1682, GenBank Acession Number: KJ778012) were selected for further analysis. The Maximum Likelihood algorithm was used to compute the best model for estimation of the revised phylogenetic tree. The revised phylogenetic tree was constructed in MEGA under the criterion of maximum likelihood using the Tamura 3-parameter model (Tamura and Nei, 1993) with gamma distribution and invariant sites (T92 + G + I) and reliability of the generated tree evaluated by bootstrapping analysis set to 500 replicates (Felsentein, 1985). The final analysis involved a total of 54 nucleotide sequences. All positions with less than 95% site coverage were eliminated. That is, fewer than 5% alignment gaps, missing data, and ambiguous bases were allowed at any position. There were a total of 1311 positions in the final dataset. *Toxoplasma gondii* sequences (GenBank Accession Numbers: EF472967 and U03070) were used as outgroup species to root the final *18S rRNA* phylogenetic tree. For construction of the *cox1* phylogenetic tree, sequences were selected from GenBank after BLAST analysis of the *S. cafferi cox1* sequence

(corresponding to positions 1 to 963, GenBank Accession Number: KJ778026). The *cox1* phylogenetic tree was constructed from 36 nucleotide sequences in MEGA under the criterion of maximum likelihood using the HKY85 model (Hasegawa et al.,1985) with gamma distribution (HKY + G) and reliability of the generated tree evaluated by bootstrapping analysis set to 500 replicates (Felsentein, 1985) All positions with less than 95% site coverage were eliminated. That is, fewer than 5% alignment gaps, missing data, and ambiguous bases were allowed at any position. There were a total of 687 positions in the final dataset. *Toxoplasma gondii* sequences (GenBank Accession Numbers: HM771689 and HM771690) were used as outgroup species to root the final *cox1* phylogenetic tree.

RESULTS

Light microscopy

Only macro sarcocysts were found in the present and retrospective study. They were up to 12 mm long and 6 mm wide and were located in the neck muscles and overlying connective tissue. They were pale yellow, and shaped like a litchi fruit stone or cashew nut and were turgid or flaccid (Fig. 1A-C). These sarcocysts could be easily separated from the host tissue. In histological sections the sarcocyst had a relatively thin ruffled basophilic cyst wall enclosing a

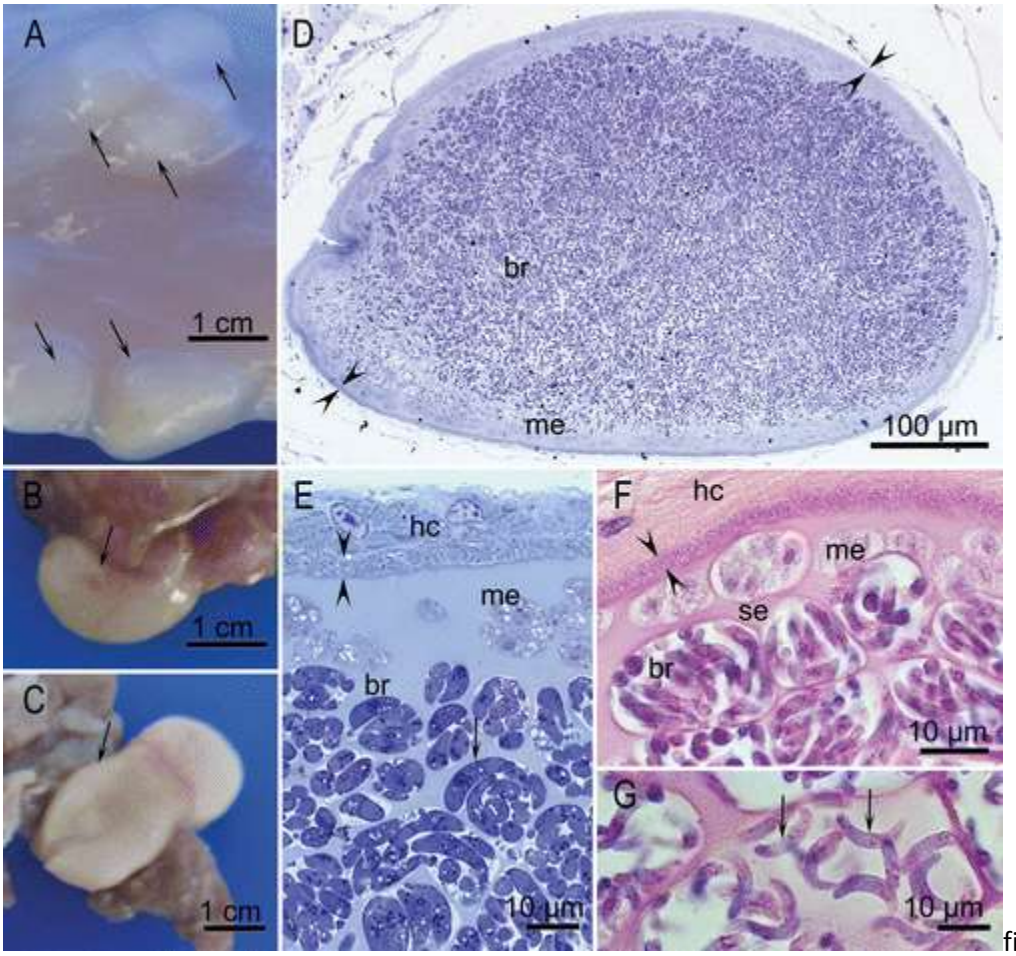

fig

Figure 1. Sarcocysts of *Sarcocystis cafferi*, n. sp. (**A, B, C**) Unstained macrocysts (arrows). . alcohol (A) or formalin (B,C) fixed. Sarcocysts are covered with connective tissue in A. (**D, E**) Sarcocysts in section stained with Toluidine blue. Note thin sarcocyst wall (opposing arrowheads) with a pale staining outer zone containing metrocytes (me), and intensely stained bradyzoites (br) in the inner part of the sarcocyst. The sarcocyst wall is not well demarcated from the host cell (hc). Arrow points to a longitudinally cut bradyzoite. (**F, G**) Section of sarcocyst stained with H and E. Note septa (se) separating groups of bradyzoites (br), and pale staining metrocytes (me). Arrows point to longitudinally cut bradyzoites.

thick layer of pale basophilic ground substance layer (gs) containing clusters of metrocytes with a central round euchromatic nucleus and moderate amount of vesicular cytoplasm and clear cell margins. The interior of the cyst was divided into round to oblong, closely packed divisions, by

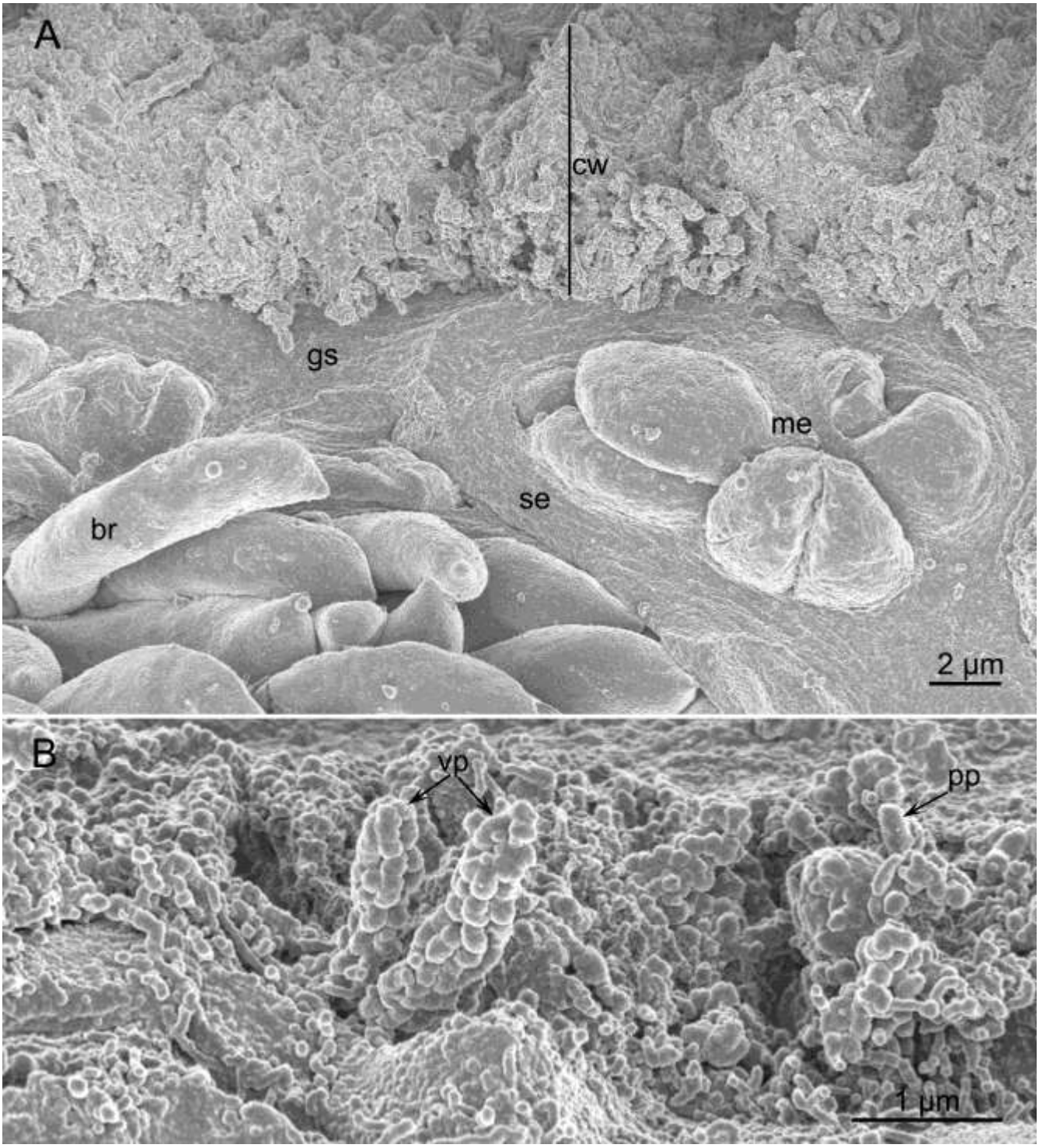

Figure 2. SEM of sectioned part of a sarcocyst. (**A)** Note highly branched combed appearance of the cyst wall (cw). The bradyzoites (br) and metrocytes (me) are arranged in sacks enclosed by thick septa (se). **(B**) Higher magnification of the cw with 2 irregularly shaped villar protrusions (vp). The vp have papillomatous structures (pp).

extensions of the gs; each division contained myriad tightly packed, slender curved bradyzoites. Cells in the central 75% of the largest cysts were necrotic. In Toluidine blue stained sections the cyst wall was not well demarcated from the host tissue (Fig. 1D-E). The sarcocyst wall was approximately 3-4 μm thick. Groups or individual metrocytes in the gs stained faintly compared with the cyst interior that contained intensely stained bradyzoites (Fig. 1E, F). Bradyzoites were banana shaped (Fig. 1E, G).

SEM

The sarcocyst wall had a mesh-like structure with irregularly shaped villar protrusions (vp) that were of different sizes and folded over the sarcocyst wall (Fig. 2A, B). The entire surfaces of vp were covered with papillomatous (pp) structures (Fig. 2B). The gs appeared granular and metrocytes were embedded in it (Fig. 2A). The pellicle of metrocytes appeared irregular. Bradyzoites were closely packed in groups, and groups were separated by thick septa. The bradyzoites were 11.5 to 14.0 μm long; their surface was uneven, and protrubances were more prominent in the non-conoidal half. The micropore was located approximately 3 μm from the tip of the pappilary conoid (Fig. 3B).The micropore had a rim, slightly raised from the surface of the bradyzoite, and had a 200 nm pore (Fig. 3B).

TEM

The sarcocyst wall was up to 3.6 μm thick and consisted of an outermost parasitophorous vacuolar membrane (pvm) that was lined by an electron dense layer (edl) approximately 25 nm thick (Fig. 4). The pvm was wavy and had out pocketing of mycelium or door stopper knobs at irregular distances (Fig. 4). These knobs were up to 115 nm long and had a free end that was up to 90 nm thick and consisted of electron dense material. The edl of the cyst wall extended along the length of the sarcocyst wall but was thin at areas of invaginations of the pvm (Fig. 4A). The

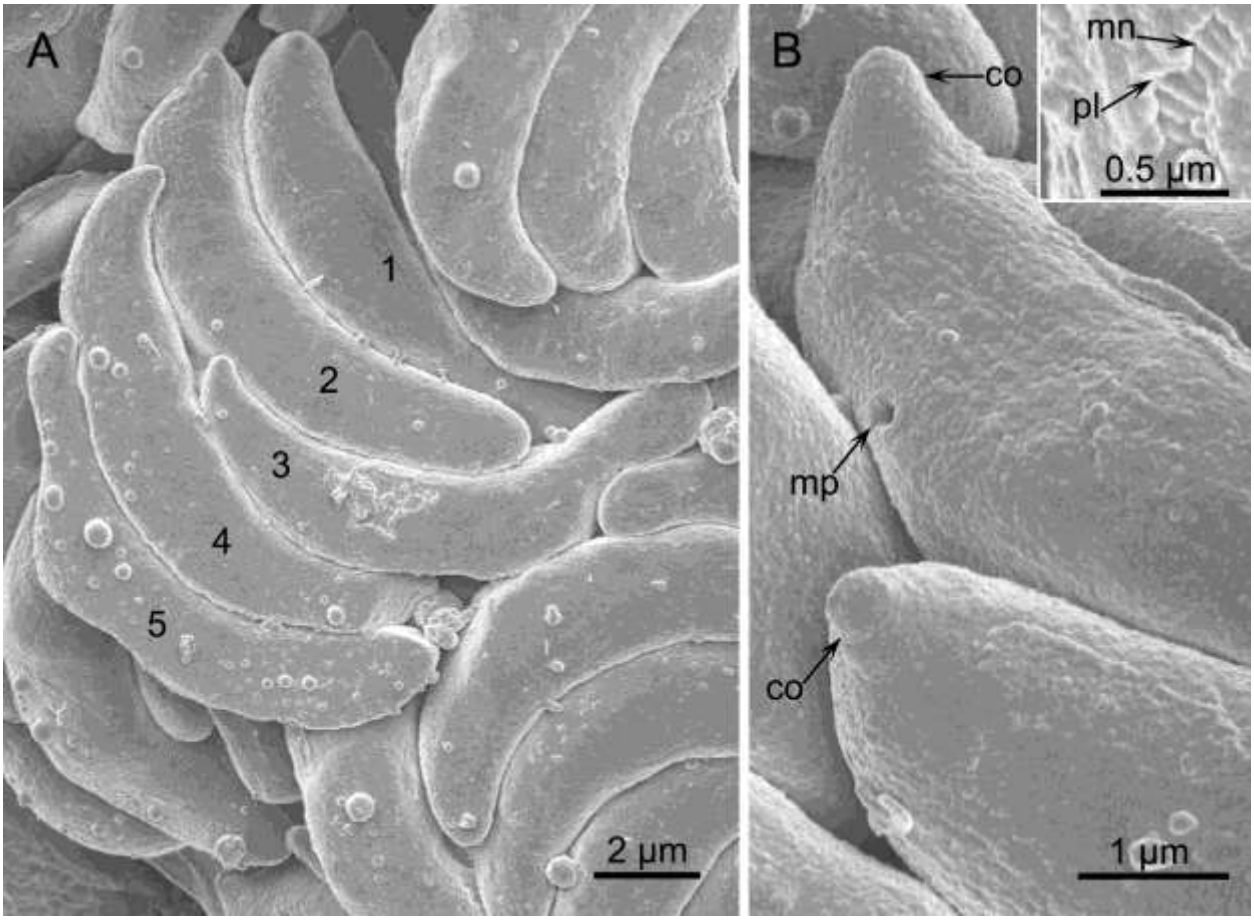

Figure 3. SEM of bradyzoites. **(A)** Note tightly packed bradyzoites . The conoidal ends of 5 bradyzoites are oriented towards the upper part of the Figure. Extraneous structures on bradyzoites are part of the cyst wall structures broken during the preparation of specimens. **(B)** Conoidal parts of 2 bradyzoites with a nipple-like conoid (co) and micropore (mp).The inset shows micronemes (mn) through the ripped part of pellicle (pl)

pvm was folded into branched projections (Fig. 4B). Some projections had a common stalk, like branches of a dead tree. These projections were up to 3 µm long, but the exact length was difficult to determine because of branching. The villar projections (vp) contained filamentous tubular structures, most of which were parallel to the long axis of the projections but some tubules criss-crossed, especially at the base (Fig. 4A). Granules were absent from these tubules.

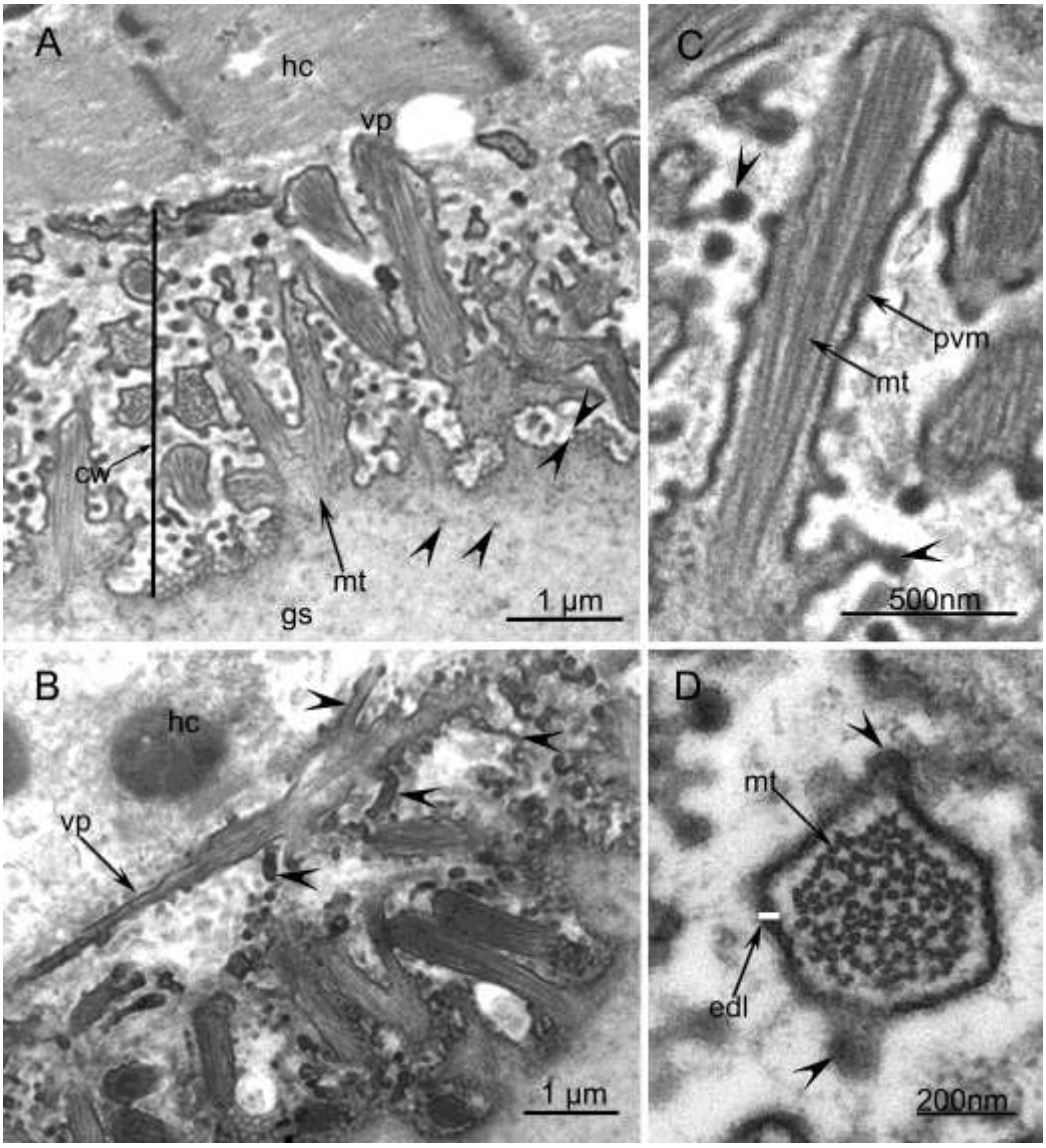

Figure 4. TEM of the sarcocyst wall of *Sarcocystis cafferi*. The parasitophorous vacuolar membrane (pvm) is undulated with numerous villar projections (vp) with out-pocketing of protrusion branches with dumbbell like ends. The microtubules (mt) are oriented longitudinally and are smooth. (**A**) The cyst wall (cw) is poorly demarcated from the host cell (hc). The pvm is invaginated at the base of villar projections (opposing arrowheads). Also note criss-crossing of mt at the base of a vp (arrow). The ground substance (gs) has few granules (arrowheads) at the junction of vp and the gs. (**B**) A highly branched vp (arrow) with out-pocketing of protrusions (arrowheads). (**C**) Longitudinal view of a vp with smooth mt. Arrowheads point to dumbbell-like endings of protrusions. (**D**) Cross section of a vp with mt cut in cross section. Also note villar protrusions (arrowheads) and electron dense layer (edl) lining the pvm.

A relatively electron lucent ground substance layer (gs) was present immediately beneath the villar projections (Figs. 4, 5). The gs immediately below the pvm contained granules, but these granules were absent from the gs extending into the interior of the cyst. Metrocytes, located in the gs, stained faintly and were often globular to oblong (Figs. 1, 5). They contained a well-defined nucleus (n), a few amylopectin granules, and few or no micronemes (Fig. 5).

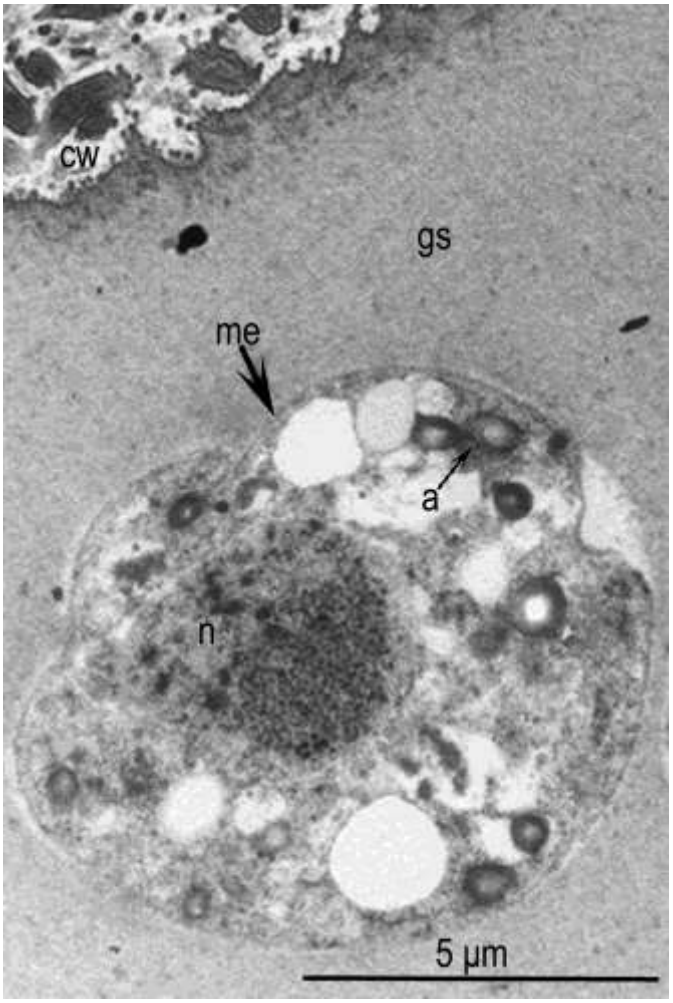

Figure 5. Ultrastructure of a metrocyte (me) in the ground substance layer (gs) underneath the cyst wall (cw). Note smooth gs and the presence of a nucleus (n), few amylopectin (a), and absence of micronemes in the metrocyte.

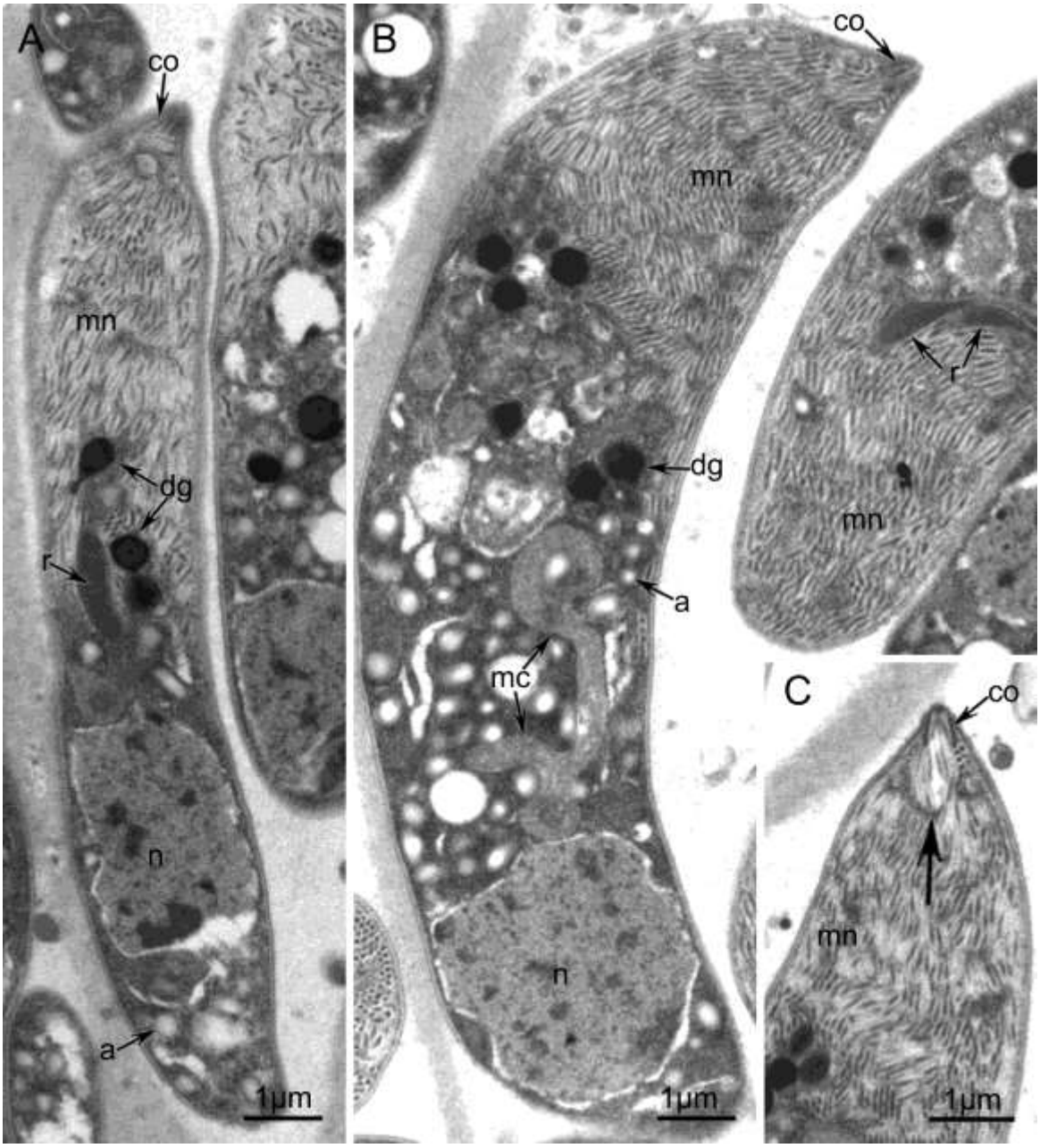

Figure 6. Ultrastrucure of bradyzoites. Note conoid (co), numerous micronemes (mn), up to 6 dense granules (dg), 1 or 2 rhoptries (r), amylopection (a), a convoluted mitrochondrion (mc), a nucleus (n).(**A**) Longitudinally cut bradyzoite with a subterminal nucleus. (**B**) Bradyzoite with a convoluted mitrochondrion but no rhoptries whereas the partially cut bradyzoite has 2 rhoptries. The nucleus appears terminal, perhaps part of the posterior end is not visible because it is cut at an angle. (**C**) Conoidal end of a bradyzoite. Note the electron dense conoid is cut longitudinally and a ring of granules surrounds the distal part of the conoid.

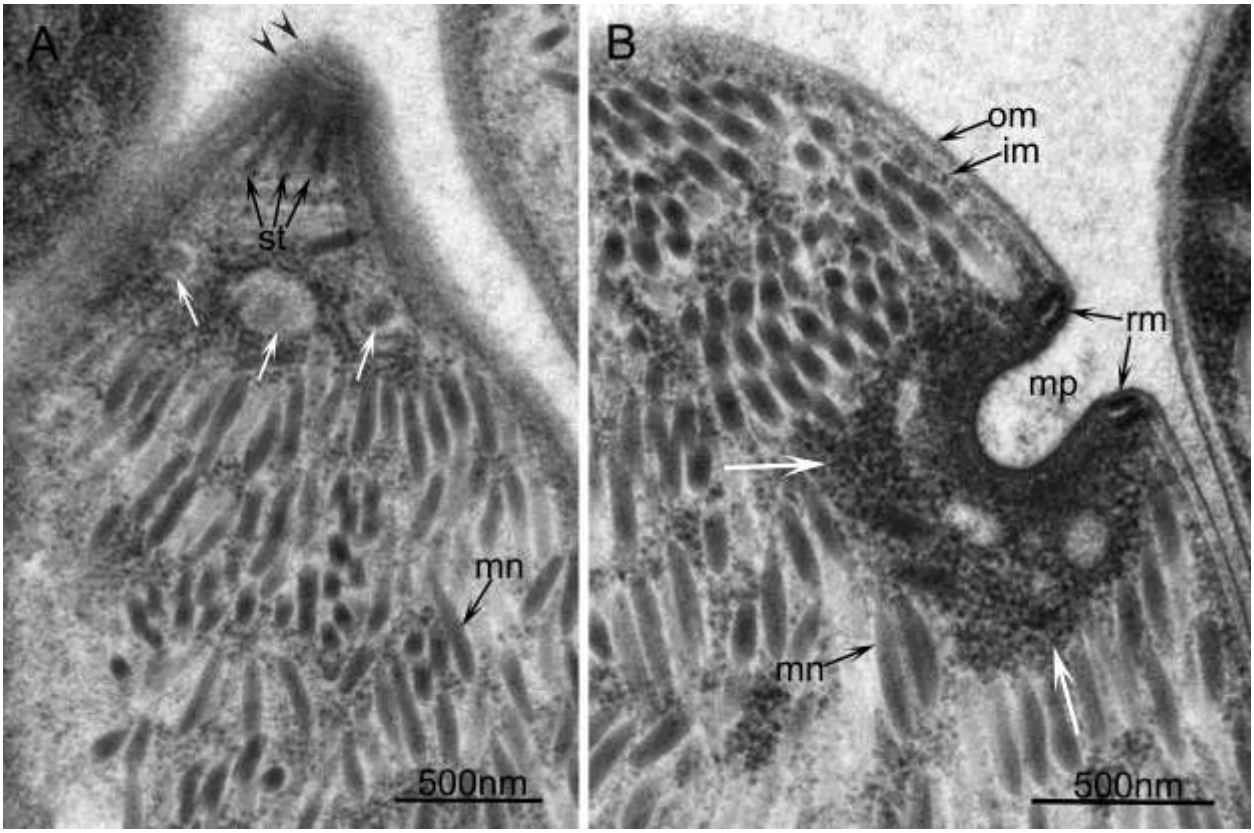

Figure 7. Portions of 2 bradyzoites at the conoidal end. (**A**) Details of conoidal end with annular and polar rings (arrowheads), sublellicular tubules (st), 3 ring like structures at the conoidal end (white arrows), and micronemes (mn). (**B**) Details of pellicle with outer (om) and inner (im) membrane at the micropore (mp) junction. The im is interrupted at the micropore opening and a rim like (rm) structure is present at the opening. Electron dense secretory material (white arrows) surround the micropore. Note numerous micronemes (mn).

Numerous bradyzoites were present below the metrocytes. They were arranged loosely or tightly in packets separated by septa (Fig. 1). Longitudinally cut bradyzoites were 12.1 x 2.7 (9.9- 14.5 x 2.1-3.2; n=12) μm in size. The bradyzoites had a double-membraned pellicle, contained a conoid, micronemes, rhoptries, amylopectin granules, dense granules, micropores, mitrochonrion, and a terminal nucleus (Figs. 6, 7). The conoid was truncated and approximately 500 x 200 nm in size. Sometimes a hollow ring with electron dense material was present below the conoid (Fig. 6). Micronemes were numerous and were dispersed throughout the anterior

half, but were most abundant in the 1/3 of the conoidal end of the parasite (Fig. 6). Micronemes were 350-375 x 50 nm in size with 1 tapering end (Fig. 7) and were arranged either in rows or haphazardly. Rhoptries had an electron dense appearance and were difficult to find in most bradyzoites. No more than 2 rhoptries (Fig. 6) were seen in any 1 plane of section; the blind bulbous end extended up to the middle of the bradyzoite. Amylopectin granules were numerous and dispersed in four-fifths of the non-conoidal end (Fig. 6). The single mitochondrion was convoluted and was nearly half the length of the bradyzoite (Fig. 6). The dense granules were approximately 50 nm in diameter and located in the conoidal part of bradyzoites. Up to 8 dense granules were seen in 1 plane of section. Micropores were up to 300 x 200 nm in size and surrounded by granular electron dense material (Fig. 7).

Molecular

The *18S1a* (~922bp) and *18S1b* (~1kb) fragments were successfully amplified by PCR from all macrocyst samples (data not shown). The *S. cafferi* partial *18s rRNA* gene sequences were deposited in GenBank (Accession numbers: KJ778010 to KJ778019). Sequence alignment of the *18S rRNA* assembly products indicated that the sequences were identical in all macrocyst samples, implying that these macrocysts belonged to the same *Sarcocystis* species.

BLAST analysis of the *S. cafferi 18S rRNA* sequence indicated 99% sequence homology with *S. fusiformis* (GenBank Accession Numbers: U03071, AF176926 and AF176927) and 97% sequence homology with *S. buffalonis* (GenBank Accession Number: AF017121). An initial maximum likelihood phylogenetic tree showed that *S. cafferi* clustered with *S. fusiformis* and *S. buffalonis* (data not shown). A revised tree also showed that *Sarcocystis cafferi* clustered with *S.*

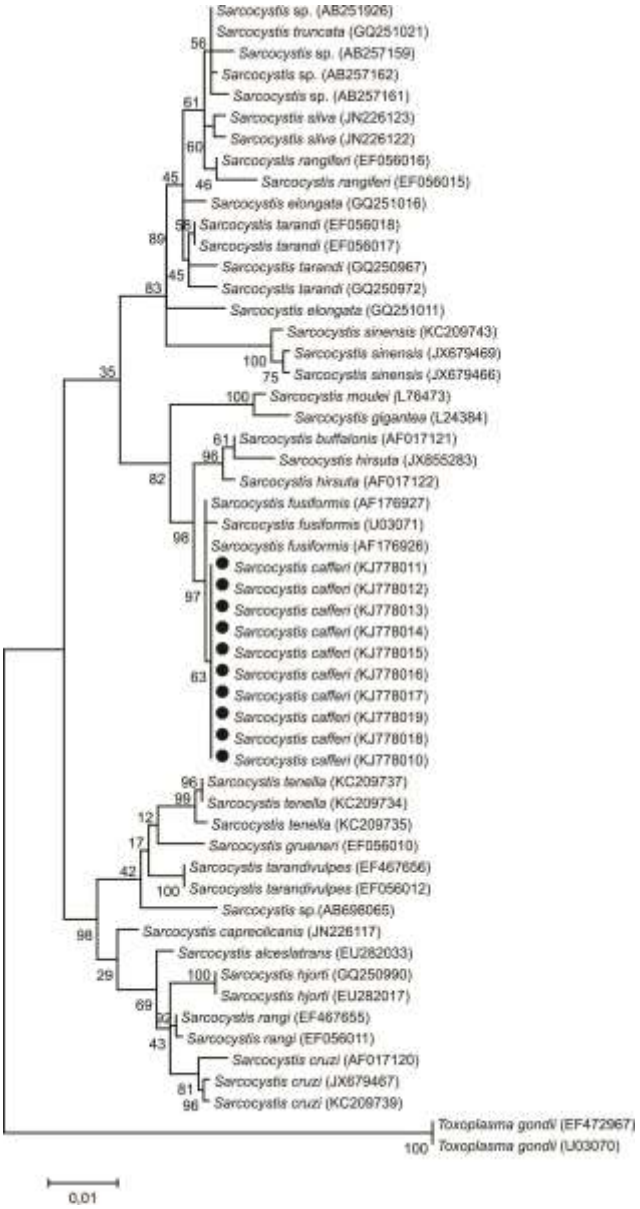

Figure 8. Maximum likelihood phylogenetic tree inferred from 52 *Sarcocystis* sp. *18S rRNA* gene sequences showing the relationship between *Sarcocystis cafferi* investigated in this study and others published in Genbank. The evolutionary history was inferred by using the Maximum Likelihood algorithm based on the Tamura 3-parameter model (T92) model with gamma distribution and invariant sites (T92 + G + I) (Tamura and Nei, 1993). The reliability of the generated tree was evaluated by bootstrapping analysis set to 500 replicates (Felsentein, 1985), percentage of trees in which the associated taxa clustered together is shown next to the branches. *Toxoplasma gondii* sequences (GenBank Accession Numbers: EF472967 and U03070) were used as outgroup species to root the final *18S rRNA* phylogenetic tree. Evolutionary analyses were conducted in MEGA5 (Tamura et al., 2011).

fusiformis, *S. buffalonis* and *S. hirsuta* (Fig. 8), indicating that these species are closely related, but *S. cafferi* appears to be more closely related to *S. fusiformis*.

The cytochrome c oxidase subunit I (*cox1*) gene was used to further investigate the relationship between *S. cafferi* and other *Sarcocystis* sp. The *cox1* gene fragment was successfully amplified from all macrocyst samples. Sequencing confirmed that the macrocysts belong to the same *Sarcocystis* species (although there were a few SNP's within the sequences) and the corresponding sequences have been deposited in GenBank (Accession numbers: KJ778020 to KJ778028). BLAST analysis of the *S. cafferi cox1* sequence indicated closest homology with *S. hirsuta* (90%; GenBank Accession Number: KC209634) and *S. gigantea* (85%; GenBank Accession Numbers: KC209601 and KC209602). However, there are no *cox1* sequences for *S. fusiformis* and *S. buffalonis* in GenBank which prevented further investigation of the genetic similarity between these two species and *S. cafferi* at the *cox1* locus. Phylogenetic analysis of the *S. cafferi cox1* gene in comparison to *Sarcocystis cox1* gene sequences selected from GenBank (after BLAST) showed that *S. cafferi* clustered with *S. hirsuta* and *S. gigantea.*

***Sarcocystis cafferi* n. sp.**

(Figs. 1-7)

Diagnosis: Only mature macroscopic sarcocysts known. Sarcocyst wall approximately 3-4 μm thick with highly branched mesh-like structure with villar protrusions that lack granules on microtubules. Bradyzoites 12.1 x 2.7 um in size with numerous micronemes and few rhoptries.

Taxonomic summary

Type host: An adult female African buffalo (*Syncerus caffer*).

Other hosts: Unknown.

Type locality: Africa

Etymology: The species is named after the host species, i.e., caffer.

Specimens deposited: ----Specimens are deposited in Smithsonian Institution, National Museum of Natural History, Washington , District of Columbia.

- USNM 1250003, *Sarcocystis cafferi,* H&E stained slide--Holotye
- USNM 1250004, *Sarcocystis cafferi,* Tol. Blue stained slide #1—Paratype1
- USNM 1250005, S*arcocystis cafferi,* Tol. Blue stained slide #2—Paratype2
- USNM 1250006, *Sarcocystis cafferi,* sarcocyst in Formalin-Voucher

DISCUSSION

There is considerable confusion concerning the identity of large sarcocysts in African buffalo. Before the recognition of more than 1 macrocysts in water buffaloes, all macrocysts had been considered *S. fusiformis* (Dubey et al., 2014). In spite of substantial differences among these ungulates, the African buffalo was also considered to harbour *S. fusiformis*. Quandt et al. (1997) first provided a full description of sarcocysts in the African buffalo and suggested that sarcocysts of the African buffalo differed from *S. fusiformis*. Sarcocysts were 2-12 mm long and up to 7 mm wide. Most sarcocysts were macroscopic, and few microscopic cysts seen in histologic sections were structurally similar to macroscopic cysts. The cyst wall contained highly branched villar protrusions (vp); the zone of Vp was 1.3-3.4 μm wide. Two types of sarcocysts were found based on the size of bradyzoites, long and short. The long bradyzoites were slender 9.4-21.3 x 1.9-3.9 μm, and the small and plump bradyzoites were 6.5-12.9 x 3.2-5.2 μm in size; these 2 types of bradyzoites never occurred in the same sarcocyst (Quandt et al., 1997). These authors indicated that sarcocysts in the African buffalo and the water buffalo were morphologically and geographically distinct. Sarcocysts in the water buffalo are fusiform in shape (hence the name fusiformis), whereas sarcocysts in the African buffalo are more oval.

Additionally, these animals belong to different genera with no evidence of inter-breeding. We propose a new name *S. cafferi* for the macroscopic sarcocyst in the African buffalo.

Sarcocystis cafferi sarcocysts differ from *S. fusiformis* of the Asian water buffalo in the following ways. Sarcocysts of *S. fusiformis* are fusiform (tapering both ends) whereas S. *cafferi* have more rounded ends. Reports of a microscopic sarcocyst in African buffalo materials could not be verified since no microscopic cysts were found in heart (92), skeletal muscle (36) and tongue (2) sections from 94 African buffalo. We therefore conclude that there is only 1 species of *Sarcocystis* in the African buffalo. Neither the paraffin blocks nor the histological slides of the tissues examined by Quandt et al. (1997) could be located. From the literature, it appears that *S. fusiformis* bradyzoites have several rhoptries (8 according to Kan and Dissanaike, 1978; 8-13 according to Ghaffar et al., 1978; 10 according to Zaman and Colley, 1972); however, only 2 rhoptries were found in *S. fusiformis* from Egypt (Dubey et al., 2014). In the present study we found only 2 rhoptries in any bradyzoite. Quandt et al. (1997) did not mention any rhoptries in their description of bradyzoites, and none are visible in illustrations. The differences in morphology and size of bradyzoites in the description by Quandt et al. (1997) and the present study are probably related to differences in the methods used to preserve and measure the sarcocysts. Bradyzoites are curved, and hence difficult to measure and their size varies with the fixative, and morphometric methods (Dubey et al., 2014b) . The vacuolar structures in the plump bradyzoites illustrated by Quandt et al. (1997) are probably degenarating bradyzoites. The present description is based on longitudinally cut bradyzoites.

Phylogenetic analysis based on *18S rRNA* gene data showed that *S. cafferi* is related to *S. buffalonis*, *S. hirsuta*, *S. gigantea* and *S. moulei* but is most closely related to *S. fusiformis* (Figs. 8). However, in the clade comprised of *S. cafferi* and *S. fusiformis* (Fig. 8), all *S. cafferi* samples

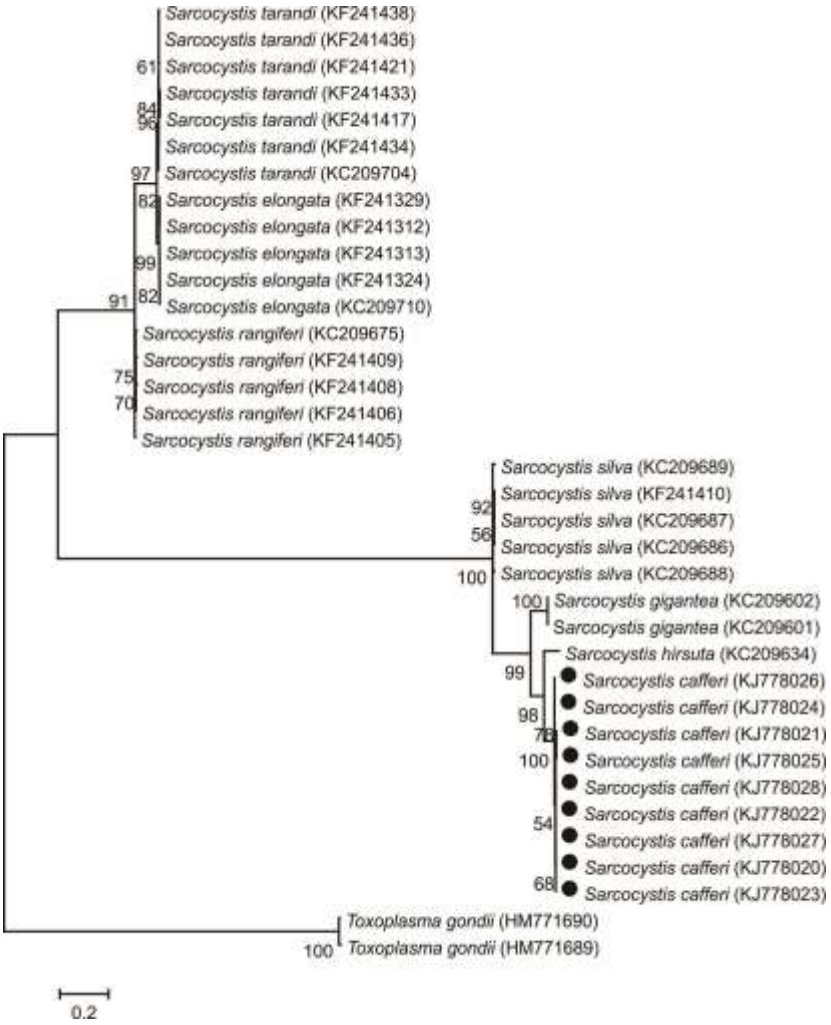

Figure 9. Maximum likelihood phylogenetic tree inferred from 36 *Sarcocystis* sp. cytochrome oxidase c subunit I (*cox1*) gene sequences showing the relationship between *Sarcocystis cafferi* investigated in this study and others published in Genbank. The evolutionary history was inferred by using the Maximum Likelihood algorithm based on the HKY85 model (Hasegawa et al., 1985) with gamma distribution (HKY + G). The reliability of the generated tree was evaluated by bootstrapping analysis set to 500 replicates (Felsentein, 1985), percentage of trees in which the associated taxa clustered together is shown next to the branches. Evolutionary analyses were conducted in MEGA5 (Tamura et al., 2011).

clustered together and were excluded in 97% of (500) bootstrap replicates from the *S. fusiformis* clade which indicates that *S. cafferi* is closely related to, but distinct from, *S. fusiformis* at this

conserved locus and may thus be a novel species. However, BLAST analysis and computation of p-distances (in MEGA) confirmed that there was very little difference between the *S. cafferi* and *S. fusiformis 18S rRNA* gene sequences, thus making definitive classification of *S. cafferi* as a new species difficult based on *18S rRNA* gene data alone. More rapidly evolving markers may be required to better resolve differences among these related parasite taxa.

To address this issue, the cytochrome c oxidase subunit 1 (*cox1*) gene was amplified and phylogenetic analysis performed which showed that *S. cafferi* is closely related to *S. gigantea* and *S. hirsuta* (Fig. 9). However, all *S. cafferi* were excluded in 98% of (500) bootstrap replicates from *S. hirsuta* in the clade comprised of *S. cafferi* and *S. hirusta* (Fig. 9). This indicates that *S. cafferi* and *S. hirsuta* are closely related but distinct.

Phylogenetic data, BLAST analysis and computation of p-distances (in MEGA) show that *S. cafferi* is not as closely related to *S. hirsuta* (via *cox1* and *18S* data) as it is to *S. fusiformis* (via *18S rRNA*). Thus, *S. cafferi* and *S. fusiformis* may be sibling species that probably diverged from a common ancestor (which itself diverged from *S. hirsuta* or the ancestor of *S. hirsuta*) since these species cannot be easily differentiated based only on *18S rRNA* or *cox1* gene data. Molecular analysis has shown *S. cafferi* is distinct from *S. hirsuta* (based on the *18S rRNA a*nd *cox1* markers) and distinct from *S. fusiformis* (based on the *18S rRNA* marker), implying that *S. cafferi* may be a novel species. At present, the lack of *cox1* sequence data for *S. fusiformis* and *S. buffalonis* prevents any definitive conclusions to be made about the phylogeny of *S. cafferi* in relation to these 2 species based on the *cox1* marker. No clear alternative marker or marker system has been generally embraced to augment what can be learned from *18S rDNA* but progress has been made in other instances by means of microsatellite loci, and/or genes encoded by the plastid and mitochondrial genomes (Asmundsson and Rosenthal, 2006; Wendte et al,

2010; Gjerde, 2013). Currently, molecular data alone cannot definitively differentiate *S. cafferi* from *S. fusiformis* however morphological data indicates that *S. cafferi* is a novel species.

Sarcocystis fusiformis, and most macrocysts of domestic and wild animals, are transmitted via felids. Furthermore, phylogenetic analysis (of both the *18S rRNA* and *cox1* markers) has shown that *S. cafferi* is closely related to *S. fusiformis* and also related to *S. buffalonis*, *S. hirsuta*, *S. gigantea* and *S. moulei* (Figs. 8, 9) which are all transmitted via felids (Gjerde, 2013). Therefore, we speculate that *S. cafferi* is likely transmitted via felids, most likely lions. The African buffalo has not been domesticated and is an abundant resident in the Kruger National Park. The buffalos can live for a long time (26 yr) and have very few predators other than lions (*Panthera leo*). Nothing is known of the life cycle of *S. cafferi* except that macrocysts occur in older animals. Because of epidemics of viral and bacterial diseases (e.g. tuberculosis, foot and mouth disease), the transport of buffalos and their tissues are strictly controlled; this imposes limitations in the study of parasites harboured by these various hosts. Nonetheless, the detailed morphological and genetic descriptions of *S. cafferi* should contribute to clarifying the diversity and relationships among this enigmatic group of parasites.

LITERATURE CITED

Asmundsson, I. M., and B. M. Rosenthal. 2006. Isolation and characterization of microsatellite markers from *Sarcocystis neurona*, a causative agent of equine protozoal myeloencephalitis. Molecular Ecology Notes **6:** 8–10.

Basson, P. A., R. M. McCully, S. P. Kruger, J. W. van Niekerk, E. Young, and V. de Vos. 1970. Parasitic and other diseases of the African buffalo in the Kruger National Park. Onderstepoort Journal of Veterinary Research **37:** 11-28.

Dubey, J. P., R. Fayer, B. M. Rosenthal, R. Calero-Bernal, and A. Uggla, A.(2014a). Identity of *Sarcocystis* species of the water buffalo (*Bubalus bubalis*) and cattle and the suppression of *Sarcocystis sinensis* as a *nomen nudum.* Veterinary Parasitology. *In press*

_____., M.Hilali, E. Van wilpe, S. K. Verma, R. Calero-Bernal, and A. Abdel-Wahab 2014b. Redescription of *Sarcocystis fusiformis* from the water buffalo (*Bubalus bubalis*). Parasitology. In press.

Dubey, J.P. C. A. Speer, and R. Fayer 1989. Sarcocystosis of animals and man. CRC Press, Boca Raton, Florida, 215 p.

_____,_____, and H. L. Shah. 1989. Ultrastructure of sarcocysts from water buffalo in India. Veterinary Parasitology **34:** 149-152.

Edgar, R. C. 2004a. Muscle: A multiple sequence alignment method with reduced time and space complexity. BMC Bioinformatics **5:** 113.

_____2004b. Muscle: Multiple sequence aligment with high accuracy and high throughput. Nucleic Acids Research **32:** 1792-1797.

Felsenstein, J. 1985. Confidence limits on phylogenies: An approach using the bootstrap. Evolution **39:** 783-791.

Ghaffar, F. A., M. Hilali, and E. Scholtyseck. 1978. Ultrastructural study of *Sarcocystis fusiformis* (Railliet,1897) infecting the Indian water buffalo (*Bubalus bubalis*) of Egypt. Tropenmedizin und Parasitologie **29:** 289-294.

Gjerde, B. 2013. Phylogenetic relationships among *Sarcocystis* species in cervids, cattle and sheep inferred from the mitochondrial cytochrome c oxidase subunit I gene. International Journal for Parasitology **43:** 579-591.

Hall, B. G. 2013. Building phylogenetic trees from molecular data with MEGA. Molecular Biology and Evolution **30:** 1229-1235.

Hasegawa, M., H. Kishino, and T. Yano. 1985. Dating of human-ape splitting by a molecular clock of mitochondrial DNA. Journal of Molecular Evolution **22:** 160-174.

Kaliner, G. 1975. Observations on the histomorphology of sarcosporidian cysts of some East African game animals (Artiodactyla). Zeitschrift für Parasitenkunde **46:** 13-23.

_____, R. Sachs, L. D. Fay, and B. Schiemann. 1971. Untersuchungen über das Vorkommen von Sarcosporidien bei ostrafikanischen Wildtieren. Zeitschrift für Tropenmedizin und Parasitologie **22:** 156-164. Please check and make certain that the Journal name is spelled correctly.

_____, J. G. Grootenhuis, and D. Protz. 1974. A survey for sarcosporidial cysts in east African game animals. Journal of Wildlife Diseases **10:** 237-238.

Kan, S. P., and A. S. Dissanaike. 1978. Studies on *Sarcocystis* in Malaysia II. Comparative ultrastructure of the cyst wall and zoites of *Sarcocystis levinei* and *Sarcocystis fusiformis* from the water buffalo, *Bubalus bubalis*. Zeitschrift für Parasitenkunde **57:** 107-116.

Medlin, L., H. J. Elwood, S. Stickel, and M. L. Sogin. 1988. The characterization of enzymatically amplified eukaryotic 16S-like rRNA-coding regions. Gene **71:** 491-499.

Quandt, S., R. G. Bengis, M. Stolte, K. Odening, and I. Bockhardt. 1997. *Sarcocystis* infection of the African buffalo *(Syncerus caffer*) in the Kruger National Park, South Africa. Acta Parasitologica **42:** 68-73.

Rosenthal, B. M., D. B. Dunams, and B. Pritt. 2008. Restricted genetic diversity in the ubiquitous cattle parasite, *Sarcocystis cruzi*. Infection, Genetics and Evolution **8:** 588-592.

Tamura, K. and M. Nei. 1993. Estimation of the number of nucleotide substitutions in the control region of mitochondrial DNA in humans and chimpanzees. Molecular Biology and Evolution **10**:512-526.

_____, D. Peterson, N. Peterson, G. Stecher, M. Nei, and S. Kumar. 2011. MEGA5: Molecular evolutionary genetics analysis using maximum likelihood, evolutionary distance, and maximum parsimony methods. Molecular Biology and Evolution **28:** 2731-2739.

Wendte, J. M., M. A. Miller, A. K. Nandra, S. M. Peat, P. R. Crosbie, P. A. Conrad, and M. E. Grigg. 2010. Limited genetic diversity among *Sarcocystis neurona* strains infecting southern sea otters precludes distinction between marine and terrestrial isolates. Veterinary Parasitology **169:** 37-44.

Yang, Z. Q., Y. X. Zuo, B. Ding, X. W. Chen, J. Luo, and Y. P. Zhang. 2001a. Identification of *Sarcocystis hominis*-like (Protozoa: Sarcocystidae) cyst in water buffalo (*Bubalus bubalis*) based on *18S rRNA* gene sequences. Journal of Parasitology **87:** 934-937.

_____,_____, Y. G. Yao, X. W. Chen, G. C. Yang, and Y. P. Zhang. 2001b. Analysis of the *18S rRNA* genes of *Sarcocystis* species suggests that the morphologically similar organisms from cattle and water buffalo should be considered the same species. Molecular and Biochemical Parasitology **115:** 283-288.

Zaman, V., and F. C. Colley. 1972. Fine structure of *Sarcocystis fusiformis* from the Indian water buffalo (*Bubalus bubalis*) in Singapore. Southeast Asian Journal of Tropical Medicine and Public Health **3:** 489-495.